Free Vibration Analysis of Laminated Composite Truncated Circular Conical Shells

Altan Kayran* and Jack R. Vinson†
University of Delaware, Newark, Delaware 19716

An analysis is presented for the free vibration characteristics of isotropic and laminated composite truncated circular conical shells including transverse shear deformation. All components of translatory and rotatory inertia are included. The applicability of linear shell theory due to Reissner is assumed, and governing equations are solved for the natural frequencies and mode shapes by using a combination of modal iteration and transfer matrix approach for different boundary conditions. Natural frequencies are compared with those predicted by the classical shell theory only for the lowest meridional mode of vibration corresponding to various circumferential wave numbers. Results indicate that the natural frequencies found by the improved shell theory equations may differ more than 50%, even for the lowest meridional mode, from the frequencies found by the classical shell theory equations depending on the boundary conditions, length, thickness, circumferential wave number, and lamination arrangement.

Nomenclature

A_c = (8,8) matrix, denotes the coefficients of classical shell theory equations
A_i = (10,10) matrix, denotes the coefficients of improved shell theory equations
$A_{ij}(i,j = 1,2,3)$ = extensional rigidity
$A_{ij}(i,j = 4,5)$ = transverse shear rigidity
$B_{ij}(i,j = 1,2,3)$ = bending-stretching coupling coefficients
c = tracer constant: takes on values 1 and 0
$D_{ij}(i,j = 1,2,3)$ = bending rigidity
E_{11},E_{22} = modulus of unidirectional composite parallel and transverse to the direction of fibers, respectively
G_{12} = inplane shear modulus of a unidirectional composite
G_{13},G_{23} = transverse shear modulus of a unidirectional composite in x-z and θ-z planes, respectively
h = thickness of the shell
$M_{xx},M_{\theta\theta},M_{x\theta}$ = moment resultants
n = circumferential wave number
N = effective tangential shear resultant
N_L = total number of lamina
$N_{xx},N_{\theta\theta},N_{x\theta}$ = membrane stress resultants
R = distance from axis of symmetry (Fig. 1)
R_{max} = radius at the large end
R_{mean} = $(R_{max} + R_{min})/2$
R_{min} = radius at the small end
R_θ = circumferential radius of curvature (Fig. 1)
Q = effective transverse shear resultant
$Q_{\theta z},Q_{xz}$ = transverse shear stress resultants
$\bar{Q}_{ij}$ = reduced stiffness coefficients of the constituent layer
SL = slant length of the cone
u_z,u_x,u_θ = displacements of the middle surface in normal, meridional, and circumferential direction
x = meridional coordinate
y_c = (8,1) matrix; denotes the fundamental variables of classical shell theory equations
y_i = (10,1) matrix; denotes the fundamental variables of improved shell theory equations
z = normal coordinate
α = cone angle
β_x,β_θ = angle of rotation of normal in meridional and tangential directions
θ = tangential coordinate
ρ = mass density
ϕ = angle between normal and axis of symmetry (Fig. 1)
ω = circular frequency

Introduction

FREE vibration analysis of truncated conical shells including transverse shear deformation has been studied by Garnet and Kemper[1] and Bacon and Bert.[2] The analysis of Garnet and Kemper was restricted to axisymmetric vibrations of isotropic conical shells. Bacon and Bert studied both isotropic and orthotropic conical shells using the Rayleigh-Ritz technique only for simply supported boundary conditions. Their analysis also did not include the study of the effect of transverse shear deformation and rotatory inertia in terms of reducing the natural frequencies from those predicted by classical shell theory. Further studies of the free vibration analysis of conical shells have been referenced by Leissa in his monograph.[3]

In the present analysis, the method includes the effects of transverse shear deformation and rotatory inertia for laminated, anisotropic composite material conical and cylindrical shells. For the classical theory, in which transverse shear deformation is neglected, the governing equations for the free vibration of laminated composite conical shells are reduced to eight first-order homogenous ordinary differential equations involving eight unknowns. For the improved theory, in which transverse shear deformation effects are included, the governing equations are reduced to ten first-order homogenous ordinary differential equations involving ten unknowns. Natural frequencies and mode shapes are found by a combination of

Received Feb. 21, 1989; revision received July 7, 1989. Copyright © 1988 American Institute of Aeronautics and Astronautics, Inc.

*Graduate Student, Department of Mechanical Engineering.
†H. Fletcher Brown Professor, Department of Mechanical Engineering. Associate Fellow AIAA.

the methods described by Kalnins[4] and Cohen,[5] in which the disadvantages of both methods are eliminated. Both methods are iterative in nature. The method of Ref. 4 requires a trial value of the frequency at each iteration step. Each step consists of obtaining eight complementary solution vectors of the homogenous system of differential equations, and comparing the determinant of a certain 4×4 matrix, depending on these solutions and the boundary conditions, with zero. This method is referred to as the frequency trial method. The method of Ref. 5 requires an estimate of displacement modes obtained from previous solution at each iteration step. Convergence is obtained when a monotonic decrease of frequency estimates, based on successive mode estimates, remains sensibly constant. This method is referred to as the mode iteration method.

In the literature, the frequency trial and mode iteration methods have only been applied to classical shell equations.[4-6] In this study, the extension of these methods to improved shell theory equations is carried out. It is noted that the inclusion of transverse shear deformation does not cause any complication for the calculation of natural frequencies and mode shapes by the above-mentioned methods.

By using the combination of the mode iteration and frequency trial methods, the effect of transverse shear deformation is studied both for isotropic and laminated conical shells. The results are obtained for different boundary conditions including nonconventional types. Different lamination arrangements that are analyzed include axial fiber laminate (all layers at 0 deg), circumferential fiber laminate (all layers at 90 deg), symmetric cross-ply and antisymmetric cross-ply. The variation of the effect of transverse shear deformation with respect to boundary conditions, thickness, length, cone angle, circumferential wave number, and different lamination arrangements is thoroughly investigated.

Geometry and Differential Equations of Free Vibration

The shell geometry and the coordinate system is defined in Fig. 1. The equations of equilibrium governing the free vibrations of a circular conical shell, written in terms of stress resultants, are[7]

$$N_{xx,x} + (N_{xx} - N_{\theta\theta})\frac{\cos\phi}{R} + N_{x\theta,\theta}\frac{1}{R} = \rho h\ddot{u}_x \tag{1}$$

$$N_{\theta\theta,\theta}\frac{1}{R} + N_{x\theta,x} + 2N_{x\theta}\frac{\cos\phi}{R} + Q_{\theta z}\frac{\sin\phi}{R} = \rho h\ddot{u}_\theta \tag{2}$$

$$Q_{\theta z,\theta}\frac{1}{R} + Q_{xz,x} + Q_{xz}\frac{\cos\phi}{R} - N_{\theta\theta}\frac{\sin\phi}{R} = \rho h\ddot{u}_z \tag{3}$$

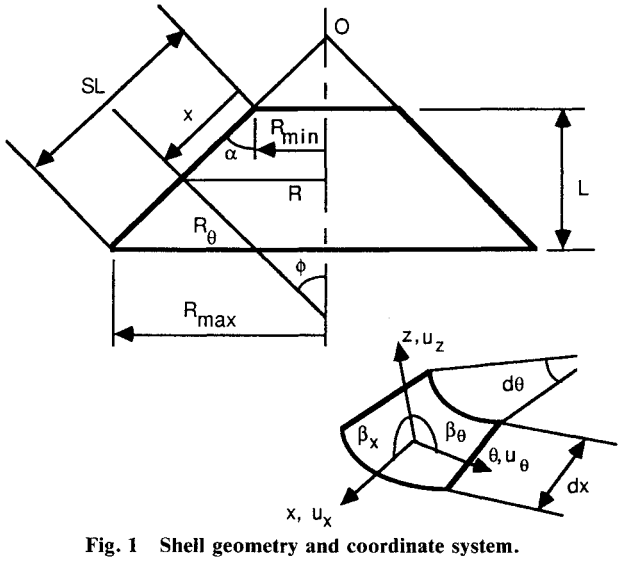

Fig. 1 Shell geometry and coordinate system.

$$M_{xx,x} + (M_{xx} - M_{\theta\theta})\frac{\cos\phi}{R} + M_{x\theta,\theta}\frac{1}{R} - Q_{xz} = \rho\frac{h^3}{12}\ddot{\beta}_x \tag{4}$$

$$M_{\theta\theta,\theta}\frac{1}{R} + 2M_{x\theta}\frac{\cos\phi}{R} + M_{x\theta,x} - Q_{\theta z} = \rho\frac{h^3}{12}\ddot{\beta}_\theta \tag{5}$$

where ".." denotes second time derivative and "," denotes partial derivative with respect to the ensuing coordinate. The stress resultant strain expressions with no stretching-shearing, twisting-shearing, bending-shearing, and bending-twisting couplings are[8]

$$N_{xx} = A_{11}\epsilon_{xx} + A_{12}\epsilon_{\theta\theta} + B_{11}\kappa_{xx} + B_{12}\kappa_{\theta\theta} \tag{6}$$

$$N_{\theta\theta} = A_{12}\epsilon_{xx} + A_{22}\epsilon_{\theta\theta} + B_{12}\kappa_{xx} + B_{22}\kappa_{\theta\theta} \tag{7}$$

$$N_{x\theta} = A_{33}\epsilon_{x\theta} + B_{33}\kappa_{x\theta} \tag{8}$$

$$M_{xx} = B_{11}\epsilon_{xx} + B_{12}\epsilon_{\theta\theta} + D_{11}\kappa_{xx} + D_{12}\kappa_{\theta\theta} \tag{9}$$

$$M_{\theta\theta} = B_{12}\epsilon_{xx} + B_{22}\epsilon_{\theta\theta} + D_{12}\kappa_{xx} + D_{22}\kappa_{\theta\theta} \tag{10}$$

$$M_{x\theta} = B_{33}\epsilon_{x\theta} + D_{33}\kappa_{x\theta} \tag{11}$$

where

$$(A_{ij},B_{ij},D_{ij}) = \sum_{k=1}^{N_L}\int_{h_{k-1}}^{h_k}\bar{Q}_{ij}^{(k)}(1,z,z^2)\mathrm{d}z, \qquad i,j = 1,2,3 \tag{12}$$

For the improved shell theory, transverse shear stress resultants Q_{xz}, $Q_{\theta z}$ are given by

$$Q_{xz} = A_{55}\epsilon_{xz} \tag{13}$$

$$Q_{\theta z} = A_{44}\epsilon_{\theta z} \tag{14}$$

where

$$(A_{44},A_{55}) = \sum_{k=1}^{N_L}\int_{h_{k-1}}^{h_k}\bar{Q}_{44}^{(k)},\bar{Q}_{55}^{(k)})f(z)\mathrm{d}z \tag{15}$$

$$f(z) = (5/4)[1 - 4(z/h)^2] \tag{16}$$

Transverse shear stiffness terms are calculated from Eq. (15), in which it is assumed that transverse shear stress has a parabolic distribution across the shell wall. A factor of 5/4 multiplies the distribution function used by Whitney,[9] so that the shear factor calculated for the layered anisotropic shell wall can be consistent with the established shear factor from the previous work by Reissner[10] and Mindlin[11] for the homogenous case. The definition of the reduced stiffness coefficients and the definition of the distances (h_k,h_{k-1}) from the midplane are explained in great detail in Refs. 8 and 12; therefore, they will not be repeated here. For a hybrid composite shell wall, the mass density ρ is calculated as an average across the thickness h, i.e.,

$$\rho = \frac{1}{h}\sum_{k=1}^{N_L}\int_{h_{k-1}}^{h_k}\rho_k\mathrm{d}\zeta \tag{17}$$

where ρ_k is the mass density of each layer which constitutes the shell wall. The strain displacement relations for a conical shell are[12]

$$\epsilon_{xx} = u_{x,x} \tag{18}$$

$$\epsilon_{\theta\theta} = \frac{1}{R}(u_{\theta,\theta} + u_x\cos\phi + u_z\sin\phi) \tag{19}$$

$$\epsilon_{x\theta} = u_{\theta,x} - u_\theta\frac{\cos\phi}{R} + u_{x,\theta}\frac{1}{R} \tag{20}$$

$$\kappa_{xx} = \beta_{x,x} \tag{21}$$

$$\kappa_{\theta\theta} = \frac{1}{R}(\beta_{\theta,\theta} + \beta_x \cos\phi) \tag{22}$$

$$\kappa_{x\theta} = \beta_{\theta,x} - \beta_\theta \frac{\cos\phi}{R} + \beta_{x,\theta}\frac{1}{R} \tag{23}$$

$$\epsilon_{xz} = \beta_x + u_{z,x} \tag{24}$$

$$\epsilon_{\theta z} = \beta_\theta - u_\theta \frac{\sin\phi}{R} + \frac{1}{R}u_{z,\theta} \tag{25}$$

For the classical theory, transverse shear strains ($\epsilon_{xz}, \epsilon_{\theta z}$) are set to zero and Eqs. (24) and (25) are used to define the respective rotations β_ϕ and β_θ in terms of the displacements u_z and u_θ. This way, for the classical theory, the total number of unknowns is reduced by two. Furthermore for the classical theory, transverse shear stress resultants Q_{xz} and $Q_{\theta z}$ are no longer given by Eqs. (13) and (14), but they are defined by the moment equilibrium Eqs. (4) and (5). Usually for the classical theory, rotatory inertia terms, which are given by the right-hand sides of Eqs. (4) and (5), are neglected and thus Q_{xz} and $Q_{\theta z}$ are given by

$$Q_{xz} = M_{xx,x} + (M_{xx} - M_{\theta\theta})\frac{\cos\phi}{R} + M_{x\theta,\theta}\frac{1}{R} \tag{26}$$

$$Q_{\theta z} = M_{\theta\theta,\theta}\frac{1}{R} + 2M_{x\theta}\frac{\cos\phi}{R} + M_{x\theta,x} \tag{27}$$

The above set of Eqs. (1–27) are the complete set of equations governing the free vibration of laminated composite conical shells for both classical and improved shell theories.

Boundary Conditions

The boundary conditions at the two rotationally symmetric ends of a shell of revolution are as follows[12]:

For the classical theory:

$$N_{xx} = 0 \quad \text{or} \quad u_x = 0 \tag{28}$$

$$M_{xx} = 0 \quad \text{or} \quad \beta_x = 0 \tag{29}$$

$$Q = 0 \quad \text{or} \quad u_z = 0 \tag{30}$$

$$N = 0 \quad \text{or} \quad u_\theta = 0 \tag{31}$$

where $Q = Q_{xz} + M_{x\theta,\theta}/R$ and $N = N_{x\theta} + M_{x\theta}\sin\phi/R$ are the effective shear stress resultants of the first and second kind, respectively.

For the improved theory:

$$N_{xx} = 0 \quad \text{or} \quad u_x = 0 \tag{32}$$

$$N_{x\theta} = 0 \quad \text{or} \quad u_\theta = 0 \tag{33}$$

$$Q_{xz} = 0 \quad \text{or} \quad u_z = 0 \tag{34}$$

$$M_{xx} = 0 \quad \text{or} \quad \beta_x = 0 \tag{35}$$

$$M_{x\theta} = 0 \quad \text{or} \quad \beta_\theta = 0 \tag{36}$$

Fundamental System of Equations

The order of the system of Eqs. (1–27) is eight with respect to x for the classical theory, and it is ten with respect to x for the improved theory. It is therefore possible to reduce Eqs. (1–27), for the classical theory, to eight first-order differential equations with respect to x involving eight unknowns and, for the improved theory, to ten first-order differential equations with respect to x involving ten unknowns. The essential point in the derivation of these equations is the definition of the variables as exactly those quantities that enter into the appropriate boundary conditions on an edge of a conical shell. The fundamental variables of the classical and improved theories are given by Eqs. (37) and (38), respectively:

$$y_c(x,\theta,t) = [u_z \; u_x \; u_\theta \; \beta_x \; Q \; N_{xx} \; N \; M_{xx}]^T \tag{37}$$

$$y_i(x,\theta,t) = [u_z \; u_x \; u_\theta \; \beta_x \; \beta_\theta \; Q_{xz} \; N_{xx} \; N_{x\theta} \; M_{xx} \; M_{x\theta}]^T \tag{38}$$

For the free vibration analysis, the dependence of each quantity on time appears in a factor $\exp(i\omega t)$, where ω is the frequency. Since, for a shell of revolution, the motion must be periodic in θ the dependence of each quantity on θ appears as a combination of $\cos n\theta$ and $\sin n\theta$, where n is the circumferential wave number. By using these facts, each quantity in the equations of motion, Eqs. (1–5), and strain displacement relations, Eqs. (18–25), is separated in time t and circumferential coordinate θ. These separated equations are then reduced to eight and ten first-order homogenous ordinary differential equations for the classical and improved theories, respectively. The fundamental system of equations for the classical and improved shell theories may be cast in matrix form as

$$y_c(x)_{,x} = A_c(n,\omega_c,x)y_c(x) \tag{39}$$

$$y_i(x)_{,x} = A_i(n,\omega_i,x)y_i(x) \tag{40}$$

The nonzero elements A_c^{ij} and A_i^{ij} of the coefficient matrices A_c and A_i are given in the Appendix. Equations (39) and (40) include all translatory and rotatory inertia components, and together with the boundary conditions form an eigenvalue problem for the force and displacement modes corresponding to the eigenvalues ω_c and ω_i for the classical and improved shell theory equations, respectively. It should be noted that the first half of the vectors $y_c(x)$ and $y_i(x)$ are the displacements, and the second half are the forces consistent with each theory.

Method of Solution

The method of solution for the natural frequencies and mode shapes of free vibration is a combination of frequency trial[4] and mode iteration[5] techniques by which the disadvantages of both methods are eliminated. Both methods are iterative and make use of the multisegment method of integration technique.[13] The primary drawback of the frequency trial method is that a priori knowledge of a frequency interval that contains the desired frequency is needed for the frequency search. Especially if the fundamental frequency for a given circumferential wave number is searched for and if there is no rough idea about the value of the fundamental frequency, very long execution times may be required in order to find the fundamental frequency. Also, it is well-known that certain shells have very closely spaced natural frequencies. Therefore in order not to miss any natural frequency, one has to be very careful in selecting the proper incremental frequency to use in the frequency search. It should also be noted that in the frequency trial method, at each trial step, eight complementary solution vectors of Eq. (39) for the classical theory, and ten complementary solution vectors of Eq. (40) for the improved theory have to be obtained. The frequency trial method on the other hand gives very accurate results for any linear shell theory that is being considered. This point is also emphasized by Krauss[14] for the numerical solution of the equations of the theory of elastic shells.

In the mode iteration method, Eqs. (39) and (40) are rewritten as

$$y_c(x)_{,x} = A_c(n,x)y_c(x) + B_c(\omega,x) \tag{41}$$

$$y_i(x)_{,x} = A_c(n,x)y_i(x) + B_i(\omega,x) \tag{42}$$

where B_c and B_i are 8×1 and 10×1 matrices which include the inertia terms. With this new form, B_c and B_i correspond to the nonhomogenous terms of Eqs. (41) and (42). In this method, since the frequency ω is put into the nonhomogenous part at each iteration, only a new particular solution is needed. Since the coefficient matrices A_c and A_i do not depend on ω, the associated complementary solution vectors do not change in the iteration process. Thus, other things being equal, one can expect a considerably shorter execution time per step in the mode method. Furthermore in this method, as it is the case for Stodola's method[15] for beams, convergence to the unknown mode with the lowest frequency is automatic. However, the mode method is sensitive to the number of segments taken in the meridional direction as required by the multisegment method of integration technique. Moreover, the shell type that is being analyzed: cylindrical, conical, etc., boundary conditions and the particular circumferential mode all affect the convergence characteristics of the mode iteration method.

In order to compare the results of both methods, the fundamental frequency of a circular cylindrical shell, which is clamped at both ends, is found by the mode iteration and frequency trial methods using classical shell equations. The results of these two methods are also compared with the experimental result of Koval and Cranch.[16] It should be noted that by making the cone angle α zero, it is possible to analyze circular cylindrical shells with the equations developed here. The shell is assumed to be isotropic with modulus of elasticity of 2.067×10^{11} Pa, thickness of 2.54×10^{-4} m, radius of 0.076 m, Poisson's ratio of 0.3, and length of 0.305 m. The circumferential wave number is taken as 5 and only five iterations are performed in the mode iteration method. The results are given in Table 1. The work of Goldberg and Bogdanoff[17] for the calculation of the axisymmetric modes and frequencies of conical shells is also duplicated. The first three axisymmetric natural frequencies for an isotropic truncated conical shell, given in Fig. 3 of Ref. 17, are found by the frequency trial and mode iteration methods. Results are compared with the results of Refs. 17 and 18 in which that author has found an analytical solution for the natural frequencies, in Table 2. Results by the mode iteration and frequency trial methods are obtained with 300 segments in the meridional direction and 20 iterations are performed in the mode iteration method. As these results show, the frequency trial method gives very accurate results as long as the shell is divided into sufficient number of segments in the meridional direction as required by the multisegment integration technique.[13] In this analysis, a computer program is prepared which combines the modal iteration and frequency trial methods, thus providing an efficient and accurate code which is free of the drawbacks of each method. In searching for a fundamental frequency for a given circumferential wave number, first the mode iteration method is employed and, without waiting on its convergence, an approximate frequency is obtained. Once this approximate frequency is found, the frequency trial method is employed and the search for the fundamental frequency is started in the vicinity of the approximate frequency found by the mode iteration method. Usually, the mode iteration method gives frequency approximations higher than the actual values. This can be seen from the results given in Tables 1 and 2. It should be noted that accuracy of the solution is due to the use of a frequency trial method which is a stepwise method as referred by Krauss.[14] It is also noted by Krauss in Chapter 10 of Ref. 14 that stepwise methods represent the simplest and most accurate approach to the numerical solution of the equations of the theory of thin elastic shells. In obtaining the results presented herein, the modal iteration technique is used to speed up the finding of the frequency region where the fundamental frequency lies. If the frequency range where the fundamental frequency lies is known beforehand, there is no definite advantage, in terms of CPU time, of employing the combination of modal iteration and frequency trial methods. Furthermore, no comparison of the CPU time is done between the scheme used here and other schemes. The primary reason for the selection of the combination of frequency trial and modal iteration methods was the simplicity and accuracy of the scheme in handling the free vibration of shells under any combination of boundary conditions. The general algorithm of the frequency trial and modal iteration methods, which are used in the analysis, follows Refs. 4 and 5, respectively. In Refs. 4 and 5, frequency trial and modal iteration methods are applied to classical shell equations. Since the inclusion of transverse shear deformation only changes the sizes of the matrices used in the solution, the general algorithm used will not be explained here. Readers are referred to Refs. 4 and 5 for the details of each method.

Table 1 Comparison of natural frequencies

Number of segments in the meridional direction	Mode iteration, Hz	Frequency trial, Hz	Result by Ref. 9, Hz
15	619	578	559
20	584	578	559
50	580	578	559
90	579	578	559

Table 2 Further comparison of natural frequencies

Mode	Analytical result by Ref. 17, Hz	Result by Ref. 18, Hz	Frequency trial, Hz	Mode iteration, Hz
1	1072	1071	1072	1132
2	1315	1315	1315	1316
3	1611	1610	1610	1615

Results and Discussion

By using the scheme described in the previous section, numerical results are obtained both for isotropic and laminated conical shells. Boundary conditions analyzed in this study are indicated in Table 3. Results are obtained only for the fundamental meridional mode corresponding to different circumfer-

Table 3 List of boundary conditions

Case no.	Description
1	Both edges simply supported without axial constraint
2	Both edges simply supported with axial constraint
3	Both edges clamped with axial constraint (fixed edges)
4	Both edges clamped without axial constraint
5	Both edges clamped without tangential constraint
6	Small edge simple (without axial constraint). Large edge fixed
7	Small edge fixed. Large edge simple (same as 6 with edges reversed)
8	Small edge fixed, large edge free

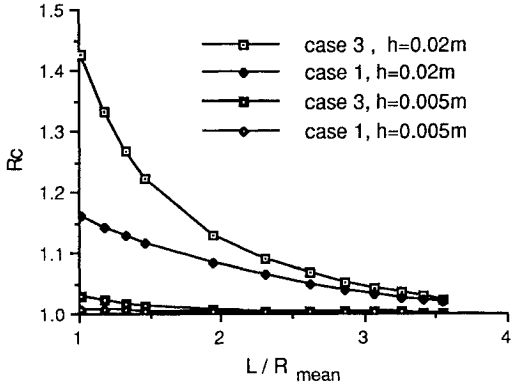

Fig. 2 Fundamental frequency ratio vs L/R_{mean} ($n = 3$, $\alpha = 20$ deg).

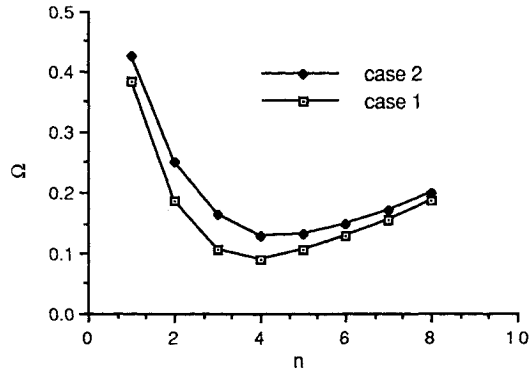

Fig. 3 Nondimensional frequency vs circumferential wave number ($h/R_{mean} = 0.013$, $SL/R_{mean} = 2.786$, $\alpha = 20$ deg).

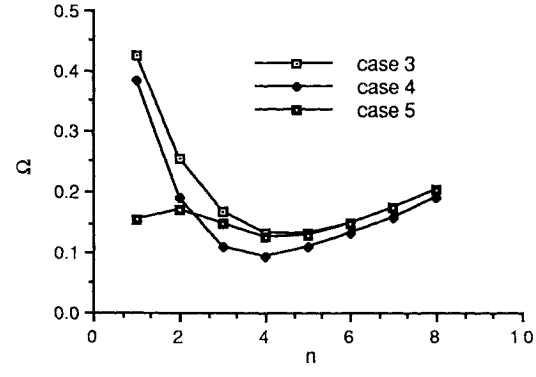

Fig. 4 Nondimensional frequency vs circumferential wave number ($h/R_{mean} = 0.013$, $SL/R_{mean} = 2.786$, $\alpha = 20$ deg).

ential wave numbers. The influence of boundary conditions, including nonconventional types, length, and cone angle was studied for isotropic conical shells. Emphasis was given to the effect of different lamination arrangements on the natural frequencies, found from the classical and improved shell theory equations, for the laminated composite conical shells.

Results for Isotropic Conical Shells

In this section, numerical results are carried out for conical shells which are made of aluminum. Material properties of aluminum that are used in the analysis are: Young's modulus $E = 7 \times 10^{10}$ Pa, Poisson's ratio $\nu = 0.33$, and mass density $\rho = 2710$ kg/m^3. In all of the calculations, the radius of the cone at the small edge is taken as 0.0508 m. In Fig. 2, the fundamental frequency ratio ($Rc = \omega_c/\omega_i$), which is defined as the ratio of the frequency found by the classical theory to the frequency found by the improved theory, is plotted against L/R_{mean} for cases 1 and 3 and different thicknesses. Results are obtained for a circumferential wave number of 3 and cone angle of 20 deg. It was found that significant differences (distinctly lower frequencies for the improved theory) occurred only for the shorter conical shells. Furthermore, as the shell thickness increases, the differences in the frequencies predicted by the classical and improved theories also increase. It was also found that the effect of transverse shear deformation in terms of reduction of the corresponding frequency due to classical theory, for a clamped-clamped shell, is greater than that for a simply supported shell.

Figures 3 and 4 compare some of the results for the nonconventional boundary conditions with the conventional ones. The ordinate in these figures is the nondimensional frequencies ($\Omega = \{[\rho(1-\nu^2)R^2_{mean}\omega_i^2]/E\}^{1/2}$) calculated using improved theory equations. Since, for the particular shell, the frequencies found by the classical theory were very close to the frequencies of the improved theory, they were not plotted. Figure 3 shows the effect of constraining the axial displacement for simply supported conical shell. It was found that the increase of the fundamental frequency due to the restraint of the axial displacement was higher at low circumferential wave numbers and this increase gradually diminished at higher circumferential modes. In Fig. 4, the effect of relaxing the axial and tangential displacement on the fundamental frequency of a clamped-clamped (case 3) shell is plotted. The effect of relaxing the axial displacement was found to be very similar to the one for the simply supported case given in Fig. 3. However, relaxing the tangential displacement ($u_\theta = 0$) significantly lowered the frequency for $n = 1$. This result was also found by Forsberg[19] for circular cylindrical shells.

Figures 5 and 6 show the effect of the cone angle α on the fundamental frequency ratio ($Rc = \omega_c/\omega_i$) for cases 1, 3, 6, and 7, respectively. Both figures are obtained for a circumferential wave number of 3. Since for $\alpha = 0$ deg h/R_{mean} is smallest, the effect of transverse shear deformation is the highest. For α greater than 50 deg, further increase of the cone angle does not have any appreciable effect on the fundamental frequency ratio.

The effect of including rotatory inertia terms in the classical shell equations is depicted in Fig. 7 for various thicknesses. In this figure, the ordinate is the ratio of the fundamental frequency calculated, where the numerator is the frequency including rotatory inertia and the denominator neglects that effect. As Fig. 7 shows, rotatory inertia terms become significant when h/R_{mean} increases. Therefore for very thin shells (small h/R_{mean}), the neglect of rotatory inertia terms does not introduce significant errors.

Results for Laminated Conical Shells

In this section, numerical results are presented for laminated conical shells, in which the lamination arrangement is restricted to the cases with bending-stretching coupling but with no stretching-shearing, twisting-shearing, bending-shearing, and bending-twisting couplings. Some commonly used lamination arrangements which correspond to these cases and which

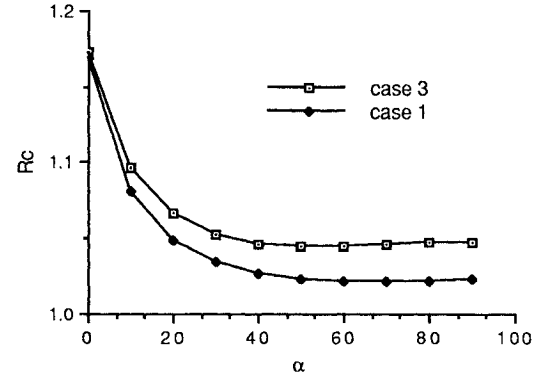

Fig. 5 Fundamental frequency ratio vs cone angle ($h = 0.02$ m, $SL = 0.27$ m, $n = 3$).

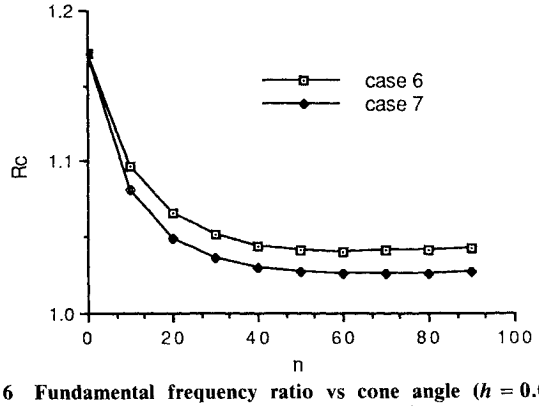

Fig. 6 Fundamental frequency ratio vs cone angle ($h = 0.02$ m, $SL = 0.27$ m, $n = 3$).

are also studied here are listed in Table 4. A material is selected containing an average of 56.1% boron fibers by volume imbedded in an epoxy matrix, resulting in a unidirectional filamentary lamina which has the following elastic constants and material properties[20]: $E_{11} = 2.24 \times 10^{11}$ Pa, $\nu_{12} = 0.256$, $E_{22} = 1.27 \times 10^{10}$ Pa, $G_{12} = G_{13} = 4.42 \times 10^{9}$ Pa, $G_{23} = 2.48 \times 10^{9}$ Pa, and $\rho = 2527$ kg/m^3.

It is noted that boron/epoxy, which has been of considerable interest in airframe applications, is an highly orthotropic material. Results are obtained for a conical shell with a cone angle of 20 deg, radius at the small end $R_{\min}$ of 0.0508 m, and slant length SL of 0.27 m. The boundary condition that is analyzed is case 3.

Figure 8 shows the effect of thickness on the fundamental frequency ratio as a function of circumferential wave number

Table 4 Characteristics of some commonly used lamination arrangements

Laminate name	Description	Stiffness characteristics
Meridionally unidirectional	All layers at 0 deg	$A_{13} = A_{23} = D_{13} = D_{23} =$ all $B_{ij} = 0$
Circumferentially unidirectional	All layers at 90 deg	$A_{13} = A_{23} = D_{13} = D_{23} =$ all $B_{ij} = 0$
Symmetric cross-ply	Alternating 0- and 90-deg layers: odd number of layers	$A_{13} = A_{23} = D_{13} = D_{23} =$ all $B_{ij} = 0$
Unsymmetric cross-ply	Alternating 0- and 90-deg layers: even number of layers	$A_{13} = A_{23} = D_{13} = D_{23} = 0$, $B_{22} = -B_{11}$ remainder $B_{ij} = 0$

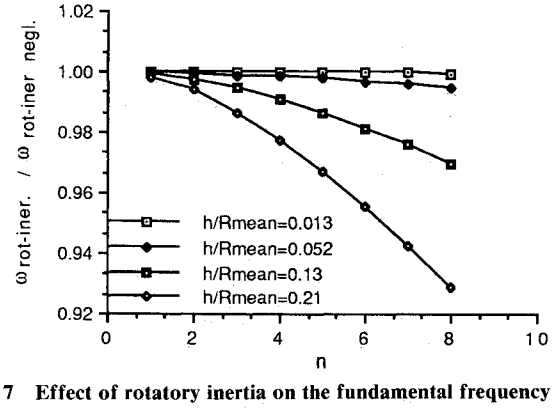

Fig. 7 Effect of rotatory inertia on the fundamental frequency (case 3, $SL/R_{\text{mean}} = 2.786$, $\alpha = 20$ deg).

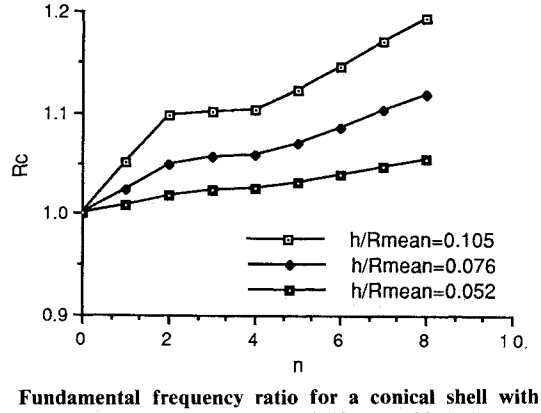

Fig. 8 Fundamental frequency ratio for a conical shell with meridional fiber orientation ($SL/R_{\text{mean}} = 2.786$, $\alpha = 20$ deg).

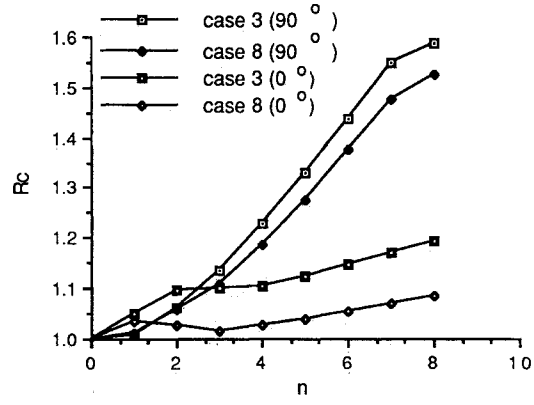

Fig. 9 Effect of different lamination arrangement on the fundamental frequency ratio ($h/R_{\text{mean}} = 0.105$, $SL/R_{\text{mean}} = 2.786$, $\alpha = 20$ deg).

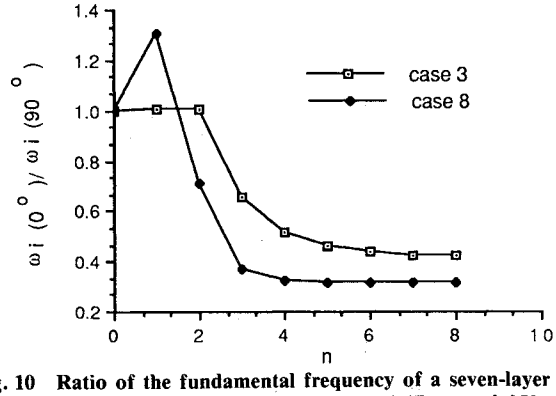

Fig. 10 Ratio of the fundamental frequency of a seven-layer 0-deg shell to a seven-layer 90-deg shell ($h/R_{\text{mean}} = 0.052$, $SL/R_{\text{mean}} = 2.786$, $\alpha = 20$ deg).

for a seven-layer-aligned parallel ply conical shell. It was found that for axisymmetric modes ($n = 0$) transverse shear deformation and the thickness did not have an appreciable effect on the fundamental frequency. Figures 9 and 10 show the effect of different lamination arrangements and the relaxing of the large end displacements on the fundamental frequency ratio of a seven-layer clamped-clamped shell. As Fig. 9 depicts, at low circumferential wave numbers the effect of transverse shear deformation is higher for a shell with axial fiber orientation (0 deg) than for a shell with circumferential fiber orientation (90 deg). However, at high circumferential wave numbers this trend is reversed. Furthermore, it was also found that relaxing the large end displacements reduces the effect of transverse shear deformation in both all-axial and all-circumferential fiber orientation cases. Figure 10 shows the ratio of the fundamental frequency (due to improved theory) of a seven-layer all-axial fiber shell to a seven-layer all-circumferential fiber shell for different circumferential wave numbers and end conditions (cases 3 and 8). In axisymmetric vibration, it was found that the orientation of the layers did not have any effect on the fundamental frequency for either end conditions. This is due to the fact that in axisymmetric motion torsional modes completely uncouple from the bending and extensional modes. For the cases analyzed, the fundamental frequency is seen to be the lowest torsional frequency. For the beam mode vibration ($n = 1$), the fundamental frequency of the axially laminated shell is higher than the circumferentially laminated shell for the clamped-free case. A slight increase was also found for the clamped-clamped case, but since the increase was very small it is not noticeable in Fig. 10. For higher circumferential wave numbers ($n > 1$), the fundamental frequency of the all-circumferential fiber case is significantly higher than for the all-axial fiber case. Physically, this is due to the higher increase of stiffness at higher circumferential wave numbers for a circumferential fiber shell than for a shell with axial fiber orientation.

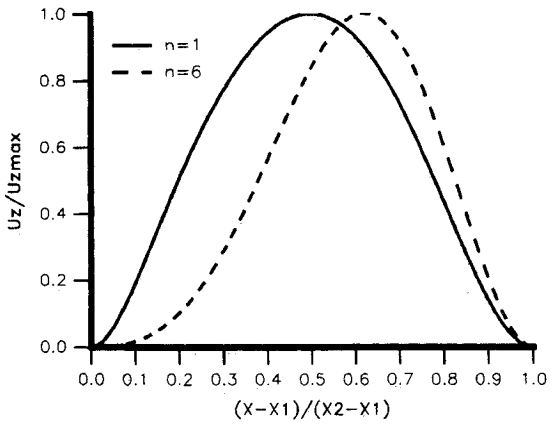

Fig. 11 Fundamental meridional mode shape of a shell with meridional fiber orientation ($h/R_{mean} = 0.052$, $SL/R_{mean} = 2.786$, $\alpha = 20$ deg).

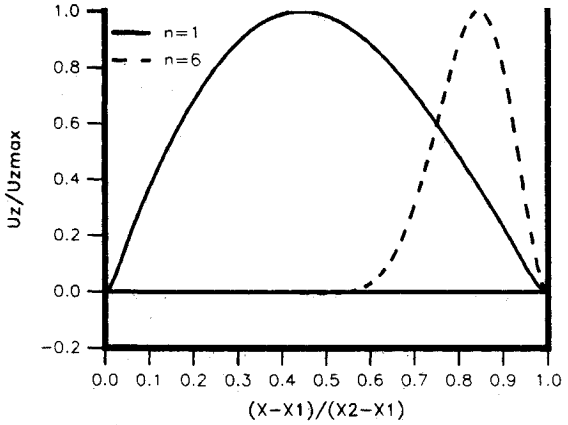

Fig. 12 Fundamental meridional mode shape of a shell with circumferential fiber orientation ($h/R_{mean} = 0.052$, $SL/R_{mean} = 2.786$, $\alpha = 20$ deg).

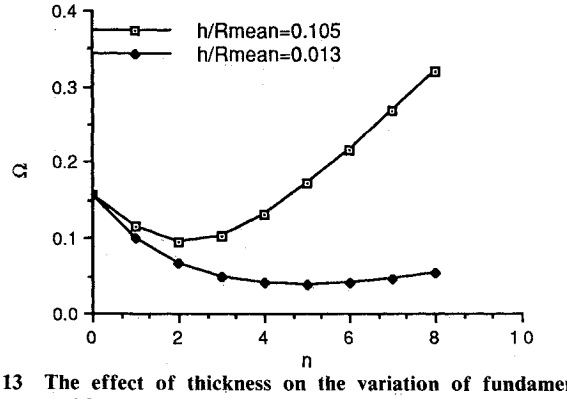

Fig. 13 The effect of thickness on the variation of fundamental frequency with respect to n (case 3, $SL/R_{mean} = 2.786$, $\alpha = 20$ deg).

Figures 11 and 12 show the transverse mode shapes for the all-axial fiber (0 deg) and the all-circumferential fiber (90 deg) cases. It is seen that there is a strong dependence of the mode shape on the circumferential wave number. In each case, the position of maximum displacement shifts toward the larger end of the shell and little transverse motion occurs at the small end with increasing circumferential wave number. Physically, the suppression of transverse displacement near the small end of the cone at high values of n is due to the short distance between consecutive nodal meridians. Thus, this results in high stiffness in this region. This suppression of transverse displacement is more pronounced for a conical shell which is stiffer in the circumferential direction than in axial direction, and this is clearly seen in Figs. 13 and 14. The shift of maximum displacement toward the larger end of the conical shell was also observed by Lindholm and Hu[21] both analytically and experimentally for isotropic conical shells.

The effect of thickness on the variation of the fundamental frequency with circumferential wave number is depicted in Fig. 13. In this figure, the ordinate is the nondimensional frequency parameter ($\Omega = \{[\rho(1-\nu^2)R^2_{mean}\omega_i^2]/E_{11}\}^{1/2}$) calculated based on the improved shell equations. As this figure shows, for thicker shells the minimum frequency occurs at lower circumferential modes than it does for thinner shells.

Figures 14 and 15 show the effect of the number of layers on the fundamental frequency ratio for symmetric cross-ply and unsymmetric cross-ply conical shell as a function of circumferential wave number. It was found that in either case, at higher circumferential wave numbers, the effect of transverse shear deformation increased with increasing number of layers. The same trend was found for unsymmetric cross-ply conical shell at low circumferential wave numbers, but for the symmetric cross-ply case transverse shear deformation effects decreased with increasing number of layers.

Finally, Fig. 16 compares the effect of transverse shear deformation for a boron/epoxy conical shell with an isotropic

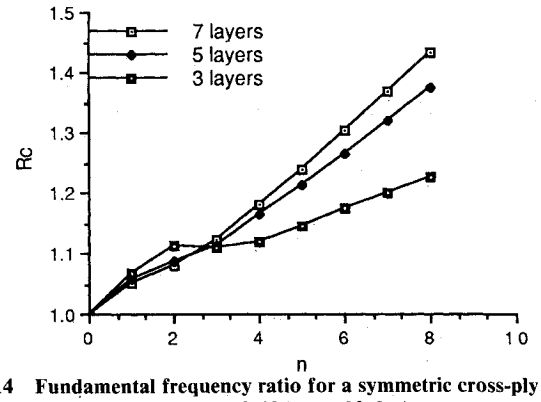

Fig. 14 Fundamental frequency ratio for a symmetric cross-ply shell ($h/R_{mean} = 0.105$, $SL/R_{mean} = 2.786$, $\alpha = 20$ deg).

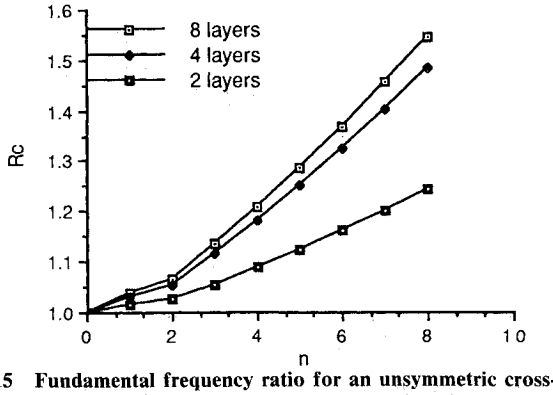

Fig. 15 Fundamental frequency ratio for an unsymmetric cross-ply shell ($h/R_{mean} = 0.105$, $SL/R_{mean} = 2.786$, $\alpha = 20$ deg).

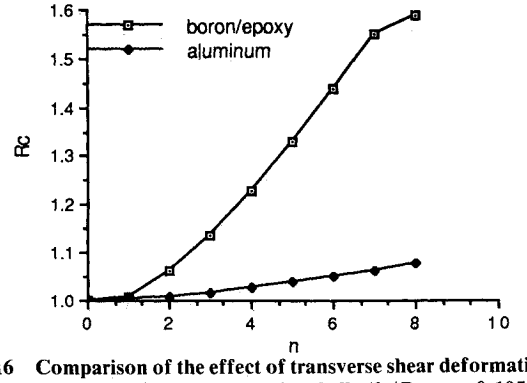

Fig. 16 Comparison of the effect of transverse shear deformation for a highly orthotropic and isotropic shell ($h/R_{mean} = 0.105$, $SL/R_{mean} = 2.786$, $\alpha = 20$ deg).

one. The boron/epoxy shell is assumed to have seven layers with all of the fibers in the circumferential direction. The isotropic material is taken as aluminum. For the shell made of boron/epoxy, transverse shear deformation effects were found to be significantly higher than for the aluminum shell as the circumferential wave number is increased.

Concluding Remarks

On the basis of the present investigation, the following conclusions can be drawn:

1) The combination of modal iteration and frequency trial methods presents a simple, efficient, and accurate approach to the numerical calculation of the natural frequencies and mode shapes of laminated conical shells. With this approach, results can be obtained for any set of boundary conditions using classical and improved shell theory equations. The details of this analysis are given in Ref. 22.

2) It should be noted that, in practical laminated composite conical shells due to geometry, the volume fraction of fibers is a function of x. In the computational procedure developed in Ref. 22, this poses no problem.

3) The effect of transverse shear deformation in terms of reducing the corresponding frequency due to classical shell theory is significant for shorter cones ($L/R_{\text{mean}} < 3.5$–4).

4) As the shell thickness is increased, the differences in the frequencies predicted by the classical and improved theories also increase.

5) Constraining the displacements at the ends of the conical shell increases the effect of transverse shear deformation.

6) Transverse shear deformation effects increase with increasing circumferential wave number. For axisymmetric torsional modes, the effect of transverse shear deformation is the least.

7) The effect of transverse shear deformation is significantly higher for a shell with fibers oriented circumferentially than for one in which all fibers are oriented meridionally for $n > 2$.

8) For $n > 2$, a conical shell with fibers oriented circumferentially has fundamental meridional frequencies which are higher than for a shell in which all fibers are oriented meridionally.

9) There is a strong dependence of the fundamental meridional mode shape on the circumferential wave number and lamination arrangement for conical shells.

10) The transverse shear deformation effect is more significant for a composite conical shell than for an isotropic one which has the identical geometry.

Appendix

The nonzero elements A_c^{ij} of the coefficient matrix A_c of the classical shell equations are

$$A_c^{14} = -1$$

$$A_c^{21} = \frac{p}{d}\frac{\sin\phi}{R} + \frac{q}{d}\frac{n^2}{R^2}$$

$$A_c^{22} = \frac{p}{d}\frac{\cos\phi}{R}$$

$$A_c^{23} = \frac{p}{d}\frac{n}{R} + \frac{q}{d}n\frac{\sin\phi}{R^2}$$

$$A_c^{24} = \frac{q}{d}\frac{\cos\phi}{R}$$

$$A_c^{26} = \frac{D_{11}}{d}$$

$$A_c^{28} = -\frac{B_{11}}{d}$$

$$A_c^{31} = 2n\frac{t}{j}\frac{\cos\phi}{R^2}$$

$$A_c^{32} = \frac{s}{j}\frac{n}{R}$$

$$A_c^{33} = \frac{1}{j}\left(s\frac{\cos\phi}{R} + t\frac{\sin 2\phi}{R^2}\right)$$

$$A_c^{34} = 2\frac{t}{j}\frac{n}{R}$$

$$A_c^{37} = \frac{1}{j}$$

$$A_c^{41} = -\frac{k}{d}\frac{n^2}{R^2} - \frac{l}{d}\frac{\sin\phi}{R}$$

$$A_c^{42} = -\frac{l}{d}\frac{\cos\phi}{R}$$

$$A_c^{43} = -\frac{l}{d}\frac{n}{R} - \frac{k}{d}n\frac{\sin\phi}{R^2}$$

$$A_c^{44} = -\frac{k}{d}\frac{\cos\phi}{R}$$

$$A_c^{46} = A_c^{28}$$

$$A_c^{48} = \frac{A_{11}}{d}$$

$$A_c^{51} = a_1\frac{\sin^2\phi}{R^2} + a_3n^2\frac{\sin\phi}{R^3} + a_2n^2\frac{\sin\phi}{R^3} + a_4\frac{n^4}{R^4} - 4n^2\frac{\cos^2\phi}{R^4}(tu - D_{33}) - \rho h\omega_c^2 - c\omega_c^2n^2\frac{\rho h^3}{12R^2}$$

$$A_c^{52} = a_1\frac{\sin 2\phi}{2R^2} + a_2n^2\frac{\cos\phi}{R^3} - \left(us\frac{n}{R} - B_{33}\frac{n}{R}\right)2n\frac{\cos\phi}{R^2}$$

$$A_c^{53} = a_1n\frac{\sin\phi}{R^2} + a_3n\frac{\sin^2\phi}{R^3} + a_2\frac{n^3}{R^3} + a_4n^3\frac{\sin\phi}{R^4} - \left[u\left(s\frac{\cos\phi}{R} - t\frac{\sin 2\phi}{R^2}\right) + \left(-B_{33} - 2D_{33}\frac{\sin\phi}{R}\right)\frac{\cos\phi}{R}\right]2n\frac{\cos\phi}{R^2} - c\rho h^3\omega_c^2n\frac{\sin\phi}{12R^2}$$

$$A_c^{54} = a_4n^2\frac{\cos\phi}{R^3} + a_3\frac{\sin 2\phi}{2R^2} - (tu - D_{33})4n^2\frac{\cos\phi}{R^3}$$

$$A_c^{55} = -\frac{\cos\phi}{R}$$

$$A_c^{56} = -\frac{p}{d}\frac{\sin\phi}{R} - \frac{q}{d}n^2\frac{1}{R^2}$$

$$A_c^{57} = -2un\frac{\cos\phi}{R^2}$$

$$A_c^{58} = \frac{k}{d}\frac{n^2}{R^2} + \frac{l}{d}\frac{\sin\phi}{R}$$

$$A_c^{61} = A_c^{52}$$

$$A_c^{62} = a_1\frac{\cos^2\phi}{R^2} + \left(us\frac{n}{R} - B_{33}\frac{n}{R}\right)\frac{\sin\phi n}{R^2} - \rho h\omega_c^2$$

$$A_c^{63} = a_3 n \frac{\sin 2\phi}{2R^3} + a_1 n \frac{\cos\phi}{R^2}$$
$$+ \left[u\left(s \frac{\cos\phi}{R} + t \frac{\sin 2\phi}{R^2} \right) \right.$$
$$\left. + \left(-B_{33} - 2D_{33} \frac{\sin\phi}{R} \right) \frac{\cos\phi}{R} \right] \frac{\sin\phi n}{R^2}$$

$$A_c^{64} = a_3 \frac{\cos^2\phi}{R^2} + \left(2ut \frac{n}{R} - 2D_{33} \frac{n}{R} \right) \frac{\sin\phi n}{R^2}$$

$$A_c^{66} = \left(-\frac{p}{d} - 1 \right) \frac{\cos\phi}{R}$$

$$A_c^{67} = \left(u \frac{\sin\phi}{R} - 1 \right) \frac{n}{R}$$

$$A_c^{68} = \frac{l}{d} \frac{\cos\phi}{R}$$

$$A_c^{71} = A_c^{53}$$

$$A_c^{72} = A_c^{63}$$

$$A_c^{73} = a_1 \frac{n^2}{R^2} + a_2 n^2 \frac{\sin\phi}{R^3} + a_3 n^2 \frac{\sin\phi}{R^3} + a_4 n^2 \frac{\sin^2\phi}{R^4} +$$
$$- \left[u\left(s \frac{\cos\phi}{R} + t \frac{\sin 2\phi}{R^2} \right) \right.$$
$$\left. + \left(-B_{33} - 2D_{33} \frac{\sin\phi}{R} \right) \frac{\cos\phi}{R} \right] \frac{\sin 2\phi}{2R^2}$$
$$- \rho h \omega_c^2 - c\rho h^3 \omega_c^2 \frac{\sin^2\phi}{12R^2}$$

$$A_c^{74} = a_3 n \frac{\cos\phi}{R^2} + a_4 n \frac{\sin 2\phi}{2R^3} + (D_{33} - ut) \frac{\sin 2\phi n}{R^3}$$

$$A_c^{76} = -\frac{q}{d} n \frac{\sin\phi}{R^2} - \frac{p}{d} \frac{n}{R}$$

$$A_c^{77} = -u \frac{\sin 2\phi}{2R^2} - 2 \frac{\cos\phi}{R}$$

$$A_c^{78} = \frac{k}{d} n \frac{\sin\phi}{R^2} + \frac{l}{d} \frac{n}{R}$$

$$A_c^{81} = A_c^{54}$$

$$A_c^{82} = A_c^{64}$$

$$A_c^{83} = A_c^{74}$$

$$A_c^{84} = a_4 \frac{\cos^2\phi}{R^2} - 4 \frac{n^2}{R^2}(ut - D_{33}) - c\rho h^3 \omega_c^2 / 12$$

$$A_c^{85} = 1$$

$$A_c^{86} = -\frac{q}{d} \frac{\cos\phi}{R}$$

$$A_c^{87} = -2u \frac{n}{R}$$

$$A_c^{88} = \left(\frac{k}{d} - 1 \right) \frac{\cos\phi}{R}$$

The nonzero elements A_i^{ij} of the coefficient matrix A_i of the improved shell equations are

$$A_i^{14} = -1$$

$$A_i^{16} = \frac{1}{A_{55}}$$

$$A_i^{21} = \frac{p}{d} \frac{\sin\phi}{R}$$

$$A_i^{22} = \frac{p}{d} \frac{\cos\phi}{R}$$

$$A_i^{23} = \frac{p}{d} \frac{n}{R}$$

$$A_i^{24} = \frac{q}{d} \frac{\cos\phi}{R}$$

$$A_i^{25} = \frac{q}{d} \frac{n}{R}$$

$$A_i^{27} = \frac{D_{11}}{d}$$

$$A_i^{29} = -\frac{B_{11}}{d}$$

$$A_i^{32} = \frac{n}{R}$$

$$A_i^{33} = \frac{\cos\phi}{R}$$

$$A_i^{38} = \frac{D_{33}}{e}$$

$$A_i^{310} = -\frac{B_{33}}{e}$$

$$A_i^{41} = -\frac{l}{d} \frac{\sin\phi}{R}$$

$$A_i^{42} = -\frac{l}{d} \frac{\cos\phi}{R}$$

$$A_i^{43} = -\frac{l}{d} \frac{n}{R}$$

$$A_i^{44} = -\frac{k}{d} \frac{\cos\phi}{R}$$

$$A_i^{45} = -\frac{k}{d} \frac{n}{R}$$

$$A_i^{47} = -\frac{B_{11}}{d}$$

$$A_i^{49} = \frac{A_{11}}{d}$$

$$A_i^{54} = \frac{n}{R}$$

$$A_i^{55} = \frac{\cos\phi}{R}$$

$$A_i^{58} = -\frac{B_{33}}{e}$$

$$A_i^{510} = \frac{A_{33}}{e}$$

$$A_i^{61} = a_1 \frac{\sin^2\phi}{R^2} + A_{44} \frac{n^2}{R^2} - \rho h \omega_i^2$$

$$A_i^{62} = a_1 \frac{\sin 2\phi}{2R^2}$$

$$A_i^{63} = a_1 n \frac{\sin\phi}{R^2} + A_{44} \frac{n}{R_\theta R}$$

$$A_i^{64} = a_3 \frac{\sin 2\phi}{2R^2}$$

$$A_i^{65} = a_3 n \frac{\sin\phi}{R^2} - A_{44} \frac{n}{R}$$

$$A_i^{66} = -\frac{\cos\phi}{R}$$

$$A_i^{67} = -\frac{p}{d} \frac{\sin\phi}{R}$$

$$A_i^{69} = -\frac{l}{d} \frac{\sin\phi}{R}$$

$$A_i^{71} = A_i^{62}$$

$$A_i^{72} = a_1 \frac{\cos^2\phi}{R^2} - \rho h \omega_i^2$$

$$A_i^{73} = a_1 n \frac{\cos\phi}{R^2}$$

$$A_i^{74} = a_3 \frac{\cos^2\phi}{R^2}$$

$$A_i^{75} = a_3 n \frac{\cos\phi}{R^2}$$

$$A_i^{77} = \left(-\frac{p}{d} - 1\right) \frac{\cos\phi}{R}$$

$$A_i^{78} = -\frac{n}{R}$$

$$A_i^{79} = \frac{l}{d} \frac{\cos\phi}{R}$$

$$A_i^{81} = A_i^{63}$$

$$A_i^{82} = A_i^{73}$$

$$A_i^{83} = a_1 \frac{n^2}{R^2} + A_{44} \frac{\sin\phi}{R_\theta R} - \rho h \omega_i^2$$

$$A_i^{84} = a_3 n \frac{\cos\phi}{R^2}$$

$$A_i^{85} = a_3 \frac{n^2}{R^2} - A_{44} \frac{\sin\phi}{R}$$

$$A_i^{87} = -\frac{p}{d} \frac{n}{R}$$

$$A_i^{88} = -2 \frac{\cos\phi}{R}$$

$$A_i^{89} = \frac{l}{d} \frac{n}{R}$$

$$A_i^{91} = A_i^{64}$$

$$A_i^{92} = A_i^{74}$$

$$A_i^{93} = A_i^{84}$$

$$A_i^{94} = a_4 \frac{\cos^2\phi}{R^2} - \rho h^3 \omega_i^2 / 12$$

$$A_i^{95} = a_4 n \frac{\cos\phi}{R^2}$$

$$A_i^{96} = 1$$

$$A_i^{97} = -\frac{q}{d} \frac{\cos\phi}{R}$$

$$A_i^{99} = \left(\frac{k}{d} - 1\right) \frac{\cos\phi}{R}$$

$$A_i^{910} = -\frac{n}{R}$$

$$A_i^{101} = A_i^{65}$$

$$A_i^{102} = A_i^{75}$$

$$A_i^{103} = A_i^{85}$$

$$A_i^{104} = A_i^{95}$$

$$A_i^{105} = a_4 \frac{n^2}{R^2} + A_{44} - \rho h^3 \omega_i^2 / 12$$

$$A_i^{107} = -\frac{q}{d} \frac{n}{R}$$

$$A_i^{109} = \frac{k}{d} \frac{n}{R}$$

$$A_i^{1010} = -2 \frac{\cos\phi}{R}$$

where

$$p = B_{12}B_{11} - A_{12}D_{11}, \qquad q = B_{11}D_{12} - B_{12}D_{11}$$

$$k = A_{11}D_{12} - B_{11}B_{12}, \qquad l = A_{11}B_{12} - B_{11}A_{12}$$

$$d = A_{11}D_{11} - B_{11}B_{11}, \qquad e = A_{33}D_{33} - B_{33}B_{33}$$

$$a_1 = \frac{p}{d}A_{12} - \frac{l}{d}B_{12} + A_{22}, \qquad a_2 = \frac{p}{d}B_{12} - \frac{l}{d}D_{12} + B_{22}$$

$$a_3 = \frac{q}{d}A_{12} - \frac{k}{d}B_{12} + B_{22}, \qquad a_4 = \frac{q}{d}B_{12} - \frac{k}{d}D_{12} + D_{22}$$

$$t = B_{33} + D_{33} \frac{\sin\phi}{R}, \qquad s = A_{33} + B_{33} \frac{\sin\phi}{R}$$

$$j = A_{33} + 2B_{33} \frac{\sin\phi}{R} + D_{33} \frac{\sin^2\phi}{R^2}, \qquad u = \left(B_{33} + D_{33} \frac{\sin\phi}{R}\right) \frac{1}{j}$$

References

[1]Garnet, H., and Kemper, J., "Axisymmetric Free Vibrations of Conical Shells," *Journal of Applied Mechanics,* Vol. 31, Sept. 1964, pp. 458–466.

[2]Bacon, M., and Bert, C. W., "Unsymmetric Free Vibrations of Orthotropic Sandwich Shells of Revolution," *AIAA Journal,* Vol. 5, March 1967, pp. 413–417.

[3]Leissa, A. W., "Vibration of Shells," NASA SP-288, 1973.
[4]Kalnins, A., "Free Vibration of Rotationally Symmetric Shells," *Journal of Acoustical Society of America,* Vol. 36, July 1964, pp. 1355-1365.
[5]Cohen, G. A., "Computer Analysis of Asymmetric Free Vibrations of Ring Stiffened Orthotropic Shells of Revolution," *AIAA Journal,* Vol. 3, May 1965, pp. 2305-2342.
[6]Irie, T., Yamada, G., and Kaneko, Y., "Natural Frequencies of Truncated Conical Shells," *Journal of Sound and Vibration,* Vol. 92, Feb. 1984, pp. 447-453.
[7]Reissner, E., "A New Derivation of the Equations for the Deformation of Elastic Shells," *American Journal of Mathematics,* Vol. 63, 1941, pp. 177-184.
[8]Vinson, J. R., and Sierakowski, R. L., *The Behavior of Structures Composed of Composite Materials,* Martinus Nijhoff, 1986, pp. 54-62.
[9]Whitney, J. M., "The Effect of Transverse Shear Deformation on the Bending of Laminated Plates," *Journal of Composite Materials,* Vol. 3, July 1969, pp. 534-547.
[10]Reissner, E., "On a Variational Theorem in Elasticity," *Journal of Mathematical Physics,* Vol. 29, 1950, pp. 90-95.
[11]Mindlin, R. D., "Influence of Rotatory Inertia and Shear on Flexural Motions of Isotropic, Elastic Plates," *Journal of Applied Mechanics,* Vol. 18, March 1951, pp. 31-38.
[12]Soedel, W., *Vibration of Shells and Plates,* Marcel Dekker, Inc., New York, 1981, pp. 41-46.
[13]Kalnins, A., "Analysis of Shells of Revolution Subjected to Symmetrical and Nonsymmetrical Loads," *Journal of Applied Mechanics,* Sept. 1964, pp. 467-476.
[14]Krauss, H., *Thin Elastic Shells,* John Wiley and Sons Inc., New York, 1967, pp. 419-460.
[15]Den Hartog, J. P., *Mechanical Vibrations,* McGraw-Hill, New York, 1956, pp. 156-162.
[16]Koval, L. R., and Cranch, E. T., "On the Free Vibrations of Thin Cylindrical Shells Subjected to an Initial Static Torque," *Proceedings of 4th U.S. National Congress of Applied Mechanics,* Berkeley, CA, 1962, pp. 107-117.
[17]Goldberg, J. E., and Bogdanoff, J. L., "On the Calculation of the Axisymmetric Modes and Frequencies of Conical Shell," *Journal of Acoustical Society of America,* Vol. 32, June 1960, pp. 738-742.
[18]Goldberg, J. E., "Axisymmetric Oscillations of Conical Shells," *Proceedings of 9th International Congress of Applied Mechanics,* Brussels, 1956, pp. 333-343.
[19]Forsberg, K., "Influence of Boundary Conditions on the Modal Characteristics of Thin Cylindrical Shells," *AIAA Journal,* Vol. 2, Dec. 1964, pp. 2150-2157.
[20]Wu, C., and Vinson, J. R., "Nonlinear Oscillations of Laminated Specially Orthotropic Plates with Clamped and Simply Supported Edges," *Journal of Acoustical Society of America,* Vol. 49, May 1971, pp. 1561-1567.
[21]Lindholm, S. U., and Hu, C. L. W., "Nonsymmetric Transverse Vibrations of Truncated Conical Shells," AIAA Symposium on Structural Dynamics and Aeroelasticity, 1965.
[22]Kayran, A., "Free Vibration Analysis of Laminated Composite Shells of Revolution Including Transverse Shear Deformation," Ph.D. Thesis, Univ. of Delaware, DE, 1989.

Recommended Reading from the AIAA Progress in Astronautics and Aeronautics Series . . . AIAA

Opportunities for Academic Research in a Low-Gravity Environment

George A. Hazelrigg and Joseph M. Reynolds, editors

The space environment provides unique characteristics for the conduct of scientific and engineering research. This text covers research in low-gravity environments and in vacuum down to 10^{-15} Torr; high resolution measurements of critical phenomena such as the lambda transition in helium; tests for the equivalence principle between gravitational and inertial mass; techniques for growing crystals in space—melt, float-zone, solution, and vapor growth—such as electro-optical and biological (protein) crystals; metals and alloys in low gravity; levitation methods and containerless processing in low gravity, including flame propagation and extinction, radiative ignition, and heterogeneous processing in auto-ignition; and the disciplines of fluid dynamics, over a wide range of topics—transport phenomena, large-scale fluid dynamic modeling, and surface-tension phenomena. Addressed mainly to research engineers and applied scientists, the book advances new ideas for scientific research, and it reviews facilities and current tests.

TO ORDER: **Write, Phone, or FAX:** AIAA c/o TASCO, 9 Jay Gould Ct., P.O. Box 753, Waldorf, MD 20604 Phone (301) 645-5643, Dept. 415 ■ FAX (301) 843-0159

Sales Tax: CA residents, 7%; DC, 6%. For shipping and handling add $4.75 for 1-4 books (call for rates for higher quanties). Orders under $50.00 must be prepaid. Foreign orders must be prepaid. Please allow 4 weeks for delivery. Prices are subject to change without notice. Returns will be accepted within 15 days.

1986 340 pp., illus. Hardback
ISBN 0-930403-18-5
AIAA Members $59.95
Nonmembers $84.95
Order Number V-108